ELSEVIER

Journal of Nuclear Materials 258–263 (1998) 452–456

journal of nuclear materials

Examination of indention geometry-constitutive behaviour relations with confocal microscopy and finite element modeling

C. Santos [c], G.R. Odette [a,b,*], G.E. Lucas [a,b], T. Yamamoto [d]

[a] *Department of Mechanical and Environmental Engineering, University of California, Santa Barbara, CA 93106-5070, USA*
[b] *Department of Chemical Engineering, University of California, Santa Barbara, CA 93106-5070, USA*
[c] *Department of Materials, University of California, Santa Barbara, CA 93106-5070, USA*
[d] *Tohoku University, Institute for Materials Research, Sendai, Japan*

Abstract

Microhardness measurements have been of general interest in irradiated materials testing as a monitor of strength changes, and the geometry of the pile-up of material around the indentation has been found to be related to the work-hardening behavior. This relationship has been further examined here. Vickers microhardness tests were performed on a variety of metal alloys including low alloy, high Cr, and austenitic stainless steels and a Nb–Ti alloy. The pile-ups around the identations were quantified using confocal microscopy techniques. In addition, the indentation process and pile-up geometry was simulated using finite element techniques and the corresponding constitutive equations for each of the test materials. The results from these methods have been used to develop an improved understanding and quantification between the pile-up geometry and the constitutive behavior of the test material.

1. Introduction

Microhardness measurements have long been used to examine changes in flow properties in metals induced by irradiation [1,2]. Microhardness affords a relatively simple test that can be applied to small volumes of irradiated material. The value of microhardness itself is related to the flow stress of the material at a fixed level of plastic strain, and hence it can be used to monitor irradiation hardening; however, the geometry of the pile-up of material around the identation has been found to be related to the work-hardening behavior – steeper pile-ups correspond to smaller work hardening [3,4].

However, earlier methods of characterizing the pile-up geometry relied on interferometry or contact profilometry which were difficult to apply and could actually damage the indentation [3,4]. More recently confocal microscopy has been identified as a technique to obtain quantitative topographs of surfaces [5]. Hence, this study was undertaken to develop methods using confocal microscopy to estimate work hardening from microhardness identation pile-ups. The results were complemented by a finite element analysis of the indentation process using constitutive laws that approximated the materials used in the experimental program.

2. Experiment and results

Six materials were used in this study. Two tempered martensitic stainless steels (F-82H and HT-9), two low alloy reactor pressure vessel steels (A302B and A533B), a low work-hardening Nb-47.5% alloy, and an AISI 302 austenitic stainless steel that was annealed at 1050°C for 1/2 h to obtain a high work-hardening material. Details of the fabrication, composition, heat treatment and other mechanical properties of these alloys are given elsewhere [6–9].

Tensile tests were performed on small flat tensile specimens at room temperature at displacement rates of 8.8×10^{-5} m/s. The data were used to obtain average work hardening coefficients of the materials. The stress–plastic strain data were reasonably fit by a single work hardening coefficient for most of the materials. The

* Corresponding author. Tel.: +1 805 893 3525; fax: +1 805 893 8651; e-mail: odette@engineering.ucsb.edu.

0022-3115/98/$19.00
PII: S0022-3115(98)00369-9

Table 1
Average work hardening coefficients for test materials

Material	Average n
F-82H	0.07
HT-9	0.11
A302B	0.12
A533B	0.11
NbTi	0.03
Annealed SS	0.29

solution annealed austenitic stainless steel, however, showed a significant difference in work hardening at low and high strains, presumably due to the onset of plasticity induced martensitic transformation at the higher strains. Nonetheless, for purposes of correlating work hardening to an indentation pile-up geometry, which represents a range of strain accumulations, an average work hardening coefficient is probably a reasonable parameter. Values of n for each material are given below in Table 1.

Vickers microhardness tests were performed with 200 g loads at ambient temperatures on specimens that had been polished through 0.03 μm Al_2O_3. Indentations were examined with confocal microscopy (CM). As described in more detail elsewhere [5], the confocal microscope is an optical microscope configured to provide a focal plane with a very shallow depth of focus. Effectively, this can optically section a surface. When the depth of focus is small relative to the height (z) variation of the surface features, the surface is illuminated only at the points where the focal plane intersects the fracture surface. By systematically changing the specimen position in z for a fixed focal length, a series of illumination patterns are obtained as a function of z. These images can be recorded digitally and used to computationally reconstruct a quantitative, three-dimensional, digital image of the surface. The resolution in x, y is of the order of 0.5 μm and it is 0.1 μm in z.

Example topographic maps are shown in Fig. 1 for the NbTi and the annealed stainless steel. Here, contour lines represent positions of constant height relative to the "zero" surface, taken as the average height of the outer boundary of the topograph. Hence, the closely packed contours around the indentation in the low work hardening NbTi represent sharp pileups that peak at about 0.4 μm. The absence of such contour lines in the high work hardening 302 SS are indicative of a low broad pile-up that peaks at less than 0.1 μm well away from the center of the indentation. The other materials, with intermediate work hardening behavior, showed intermediate pile-up geometries.

Since the pileups were not symmetric about the hardness indentation perimeter, averaging techniques were used to obtain consistent quantitative pile-up profiles. Two averages were taken. The first averaged

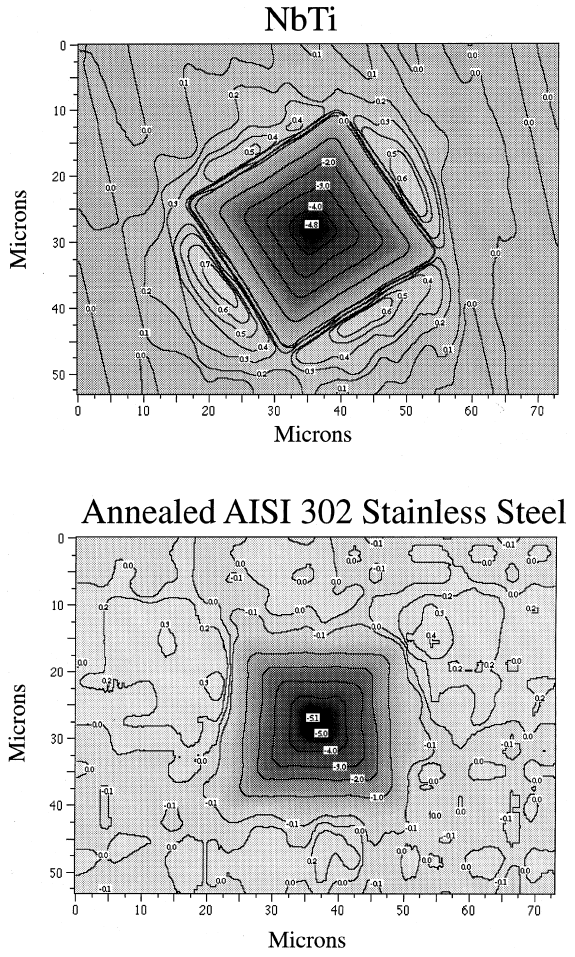

Fig. 1. Contour plots of regions around indentations in (a) NbTi and (b) annealed AISI 302 stainless steel.

depth profiles of the pile-up and indentation along directions orthogonal to one side of the indentation over the full width of the indentation. The second averaged depth profiles of the pile-up and indentation along directions orthogonal to one side of the indentation over the middle half of one side of the indentation. Hence, four averaged full length and four averaged half length profiles could be obtained for each indention. These in turn could be averaged for all of the indentation on a given material (typically five indentations). Fig. 2 compares these fully averaged profiles for all of the materials tested.

To correlate pile-up geometry with work hardening, various geometric features of the averaged indentation and pile-up profile were considered and quantified. These are illustrated in Fig. 3. As noted previously, the "zero" plane at the outer boundary of the profile. Intersections of the profile with this "zero" plane were used to define several parameters. The first intersection

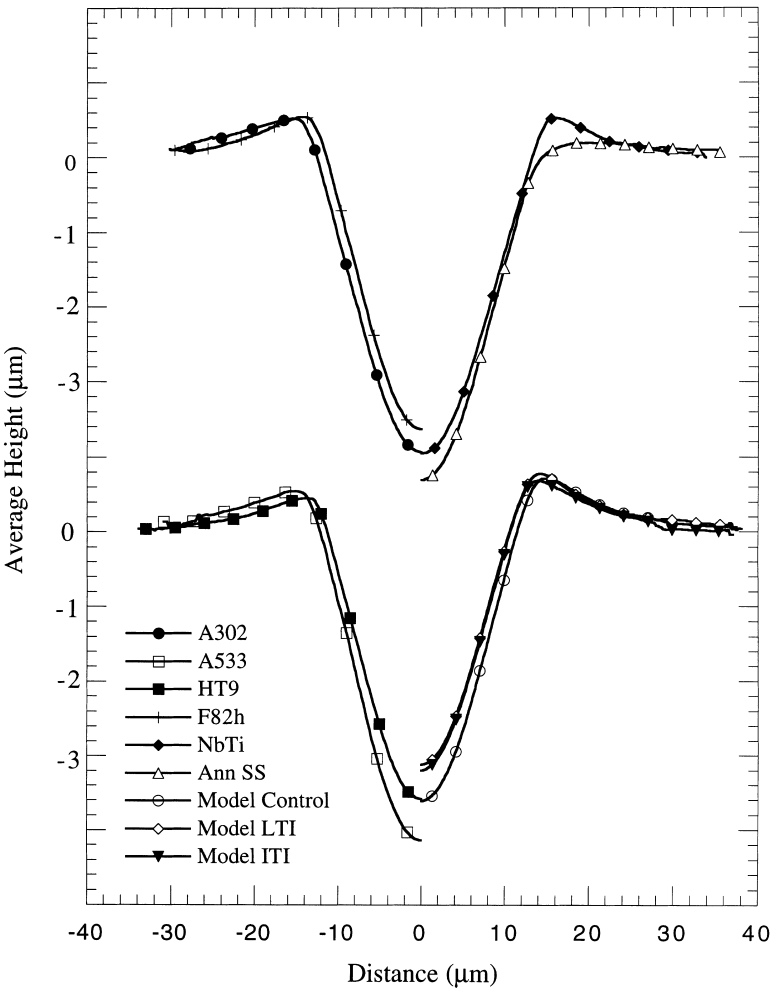

Fig. 2. Full length averaged profiles of the indentation and pile up regions in each of the materials tested in this study.

is at the outer edge of the indentation. Beyond this the pile-up profile peaked and then gradually approached the "zero" plane. Since it was difficult to identify the exact location of the second intersection of the profile with this plane, the slope of the profile in the linear region past the peak was extrapolated to the "zero" plane to obtain a second intersection. Hence, the parameters quantified included: (1) the height of the pile-up peak above the "zero" plane, h_p; (2) the depth of the indentation, h_d; (3) the distance from the center of the indentation to the first intersection of the profile with the "zero" plane, L_{M0}; (4) the distance between intersections of the profile with the "zero" plane, L_{00}; and (5) the distance from the pile-up peak position to the second intersection, L_{P0}.

A variety of correlations were examined. The best correlation was found between n and the ratio h_p/L_{00}. This is illustrated in Fig. 4. An approximate linear fit was found for all the data, but the NbTi datum lies below and the 302SS lies above the trend line for the steels.

3. Finite element analysis

Three dimensional finite element analyses of the Vickers indentation process were performed with the ABAQUS [10] to assist in understanding the indentation and pile-up formation processes. The analyses were performed with 1/8 symmetry, using 8 to 28-noded brick elements, which were highly refined near the indentation and pile-up. The mesh is illustrated in Fig. 5. The simulations were run to terminal loads of 200 g with material constitutive equations that approximated the materials of interest, using the form $\sigma = K\varepsilon^n$ for the plastic strain contribution. The indenter was modeled as a rigid indenter and a range of coefficients of friction between the indenter and material were considered.

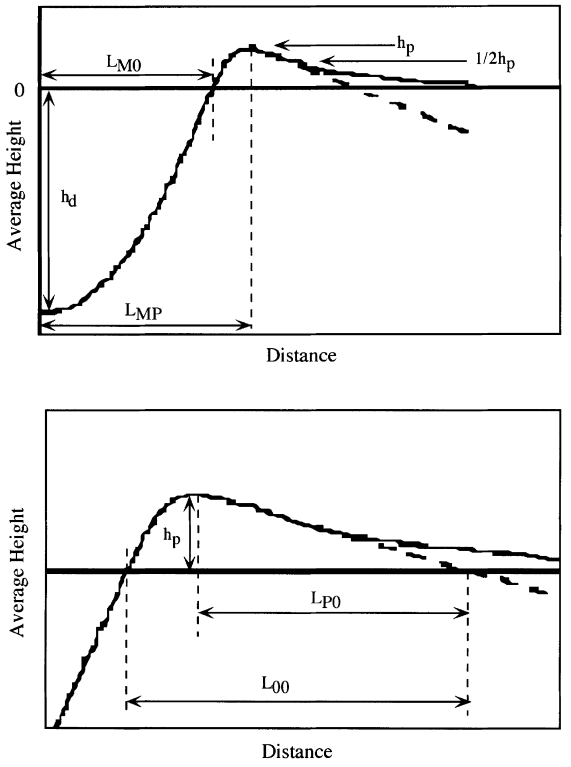

Fig. 3. Schematic illustration of the parameters defined to quantify the geometry of the indentation and pile-up for correlation with work hardening exponent.

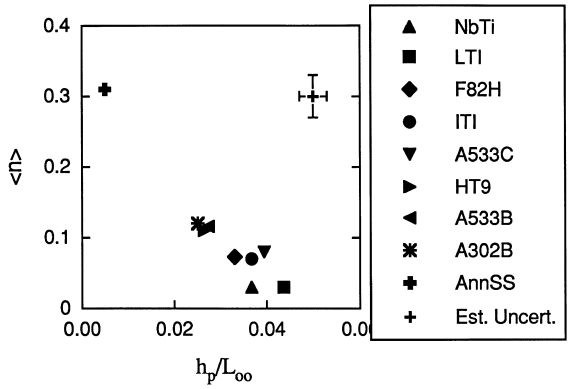

Fig. 4. Correlation of work hardening exponent with the ratio h_p/L_{00}. The solid line represents a fit to all of the data, and the dashed line a fit to the steels.

The profiles obtained were similar to the experimental trends, with low values of n giving rise to high, narrow pile-ups and high values of n giving rise to low, broad pile-ups. However, the FEM profiles tended to be more sharply peaked than the experimental profiles, and hence values of h_p/L_{00} were greater for a given n in the FEM profiles. This is illustrated in Fig. 6. However, this may be a result of the somewhat limited resolution of the confocal microscope ($\sim$0.1 μm in z). That is the exact peak height of the measured pile-up may be less (by the resolution in CM) than the actual height; likewise, and for the same reason, the slope in the linear region of the pile-up obtained by CM may be less than the actual slope. To account for this, the solid line in Fig. 5 adjusts the values of h_p and L_{00} by the following amounts, consistent with the impacts of CM resolution:

$$h_{pe} = 0.8h_{pFEM},$$

$$L_{00e} = L_{00Fem} + 2.5h_{pFEM}.$$

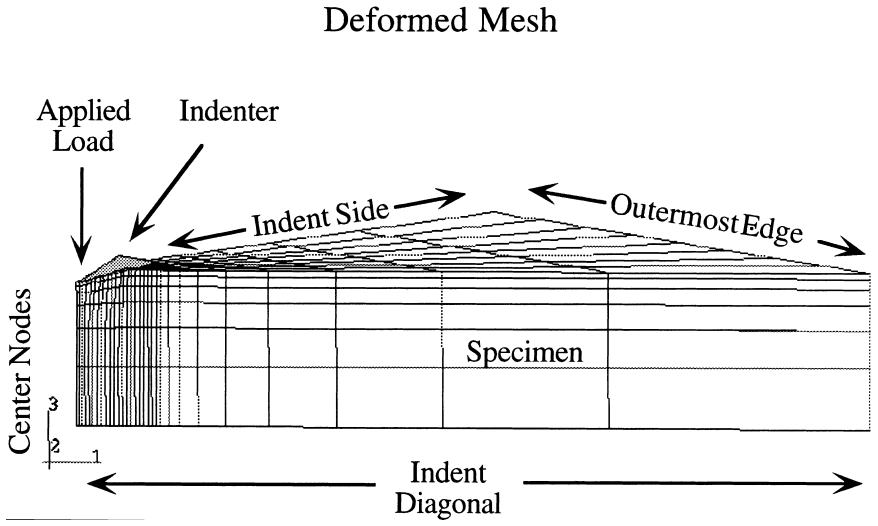

Fig. 5. Illustration of the mesh used in finite element analyses of the Vickers identation process.

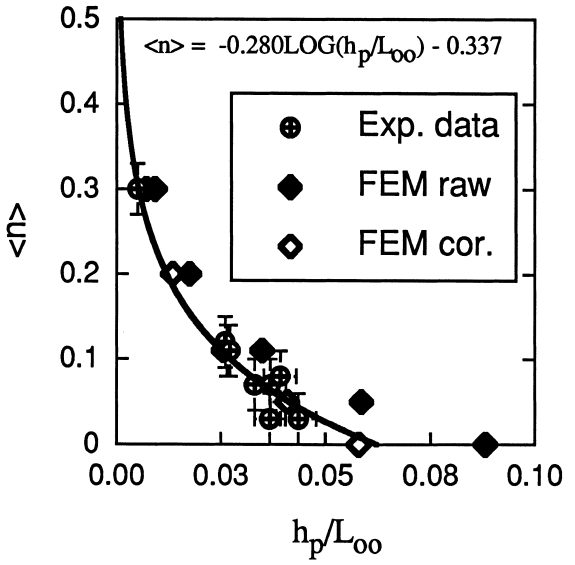

Fig. 6. Variation of the pile-up aspect ratio h_p/L_{00} with n, as determined by experiment, FEM and a modification of the FEM results to account for resolution limits in CM.

The agreement of this "corrected" curve with the experimental data is quite good.

4. Conclusions

Vickers indentation pile-up profiles reflect post-yield work hardening behavior in a variety of metals. The peak pile-up height h_p divided by the distance between points where the pile-up/indentation profile intersect the "zero" plane, L_{00}, best correlate the work hardening exponent, n, for the materials investigated. These include a variety of alloy and low alloy steels, as well as a high work hardening, solution annealed austenitic stainless steel and a low work hardening NbTi alloy. Finite element simulations of the indentation pile-up process is in general agreement with experimental observations, especially when resolution limits of the confocal microscope are incorporated.

Future measurements and modeling will confirm and extend these results and may lead to a simpler way to measure the post-yield constitutive behavior of material of interest from indentation testing.

Acknowledgements

This work was supported in part by the Office of Fusion Energy, DOE, Grant No. DE-FG03-87ER-52143. The assistance of Brian Schroeder is gratefully acknowledged.

References

[1] G.E. Lucas, G.R. Odette, Proceedings of the Conference on Nucl. Power Plant Aging, Availability Factor, and Reliability Analysis, ASM, Metals Park, OH, 1986.
[2] G.E. Lucas, Met. Trans. 21A (1990) 1105.
[3] F. Haggag, G.E. Lucas, Met. Trans. 14A (1983) 1607.
[4] M. Jayakumar, G.E. Lucas, J. Nucl. Mater. 122&123 (1984) 840.
[5] K. Edsinger, PhD thesis, Department of Chemical Engineering, UCSB, 1996.
[6] G.R. Odette, G.E. Lucas, R. Maiti, J.W. Sheckherd, J. Nucl. Mater. 122/123 (1984) 442.
[7] G.E. Lucas, G.R. Odette, K. Edsinger, B. Wirth, J.W. Sheckherd, ASTM-STP-1270, American Society for Testing and Materials, Philadelphia, PA, 1996, p. 790.
[8] G.R. Odette, G.E. Lucas, Irradiation embrittlement of LWR pressure vessel steels, EPRI NP-6114, 1989.
[9] M. Johnson, MS thesis, Department of Materials, UCSB, 1994.
[10] Hibbit, Karlsson and Sorensen, Inc., ABAQUS Users Manual, version 5.2, 1992.